JOC The Journal of Organic Chemistry

Article

pubs.acs.org/joc

Photochemistry of 1- and 2-Methyl-5-aminotetrazoles: Structural Effects on Reaction Pathways

A. Ismael,[†,‡] R. Fausto,*[,‡] and M. L. S. Cristiano*[,†]

[†]CCMAR and Department of Chemistry and Pharmacy, F.C.T., University of Algarve, P-8005-039 Faro, Portugal

[‡]CQC, Department of Chemistry, University of Coimbra, P-3004-535 Coimbra, Portugal

Supporting Information

ABSTRACT: The influence of the position of the methyl substituent in 1- and 2-methyl-substituted 5-aminotetrazoles on the photochemistry of these molecules is evaluated. The two compounds were isolated in an argon matrix (15 K) and the matrix was subjected to *in situ* narrowband UV excitation at different wavelengths, which induce selectively photochemical transformations of different species (reactants and initially formed photoproducts). The progress of the reactions was followed by infrared spectroscopy, supported by quantum chemical calculations. It is shown that the photochemistries of the two isomers, 1-methyl-(1*H*)-tetrazole-5-amine (**1a**) and 2-methyl-(2*H*)-tetrazole-5-amine (**1b**), although resulting in a common intermediate diazirine **3**, which undergoes subsequent photoconversion into 1-amino-3-methylcarbodiimide ($H_2N{-}N{=}C{=}N{-}CH_3$), show marked differences: formation of the amino cyanamide **4** ($H_2N{-}N(CH_3){-}C{\equiv}N$) is only observed from the photocleavage of the isomer **1a**, whereas formation of the nitrile imine **2** ($H_2N{-}C^{-}{=}N^{+}{=}N{-}CH_3$) is only obtained from photolysis of **1b**. The exclusive formation of nitrile imine from the isomer **1b** points to the possibility that only the 2*H*-tetrazoles forms can give a direct access to nitrile imines, while observation of the amino cyanamide **4** represents a novel reaction pathway in the photochemistry of tetrazoles and seems to be characteristic of 1*H*-tetrazoles. The structural and vibrational characterization of both reactants and photoproducts has been undertaken.

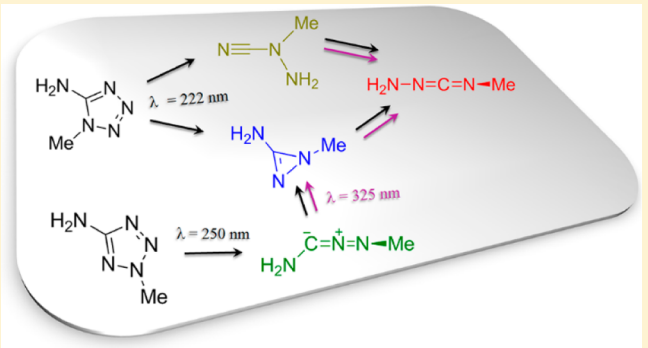

INTRODUCTION

After many decades of intense research on the structure, chemical properties, reactivity, and applications of tetrazoles, the scientific interest in the tetrazole chemotype remains perennial. In the past few years another major application of tetrazoles came to light, with the tetrazole-based photoclick chemistry providing a powerful tool for proteome profiling in living cells.[1−3] To this aim, several 2,5-disubstituted tetrazoles served as starting materials for *in situ* generation of nitrile imine dipolar species, through UV-induced photocleavage of the tetrazole, via extrusion of N_2. The nitrile imine dipolar species then react with an alkene dipolarophile, through a 1,3-dipolar cycloaddition reaction.[4−10] Of course, these and other applications of tetrazoles involving light-induced processes rely on their photochemistry, with a deeper understanding enabling the design of better systems.

The photochemistry of tetrazole itself was studied for the first time by Maier et al.[11] Primary and secondary processes were observed, leading to different photoproducts, such as nitrile imine, carbodiimide, cyanamide, and hydrogen cyanide. During the past decade, the photoreactivity of a range of tetrazole derivatives has been widely investigated, in solution and in the rigid environment of solid matrices, resulting in a wealth of information that unraveled the potential of tetrazoles as precursors of a wide variety of new scaffolds, through photolysis.[12,13]

More recently, several studies on the photolysis of tetrazoles under low-temperature matrix-isolation conditions were focused on the efficient generation, capture and characterization of unstable nitrile imines.[14−19] It was postulated from these studies that substituents play a major role on the structural characteristics of nitrile imines, this being particularly noticeable by the νCNN antisymmetric stretching infrared (IR) absorption of the nitrile imine moiety, which appears over a wide range of frequencies (2000−2250 cm^{-1}).[15,19] It was proposed that nitrile imines with IR absorptions above 2200 cm^{-1} have essentially propargylic character, possessing a CN triple bond, while those with IR absorptions below ca. 2200 cm^{-1} are more likely to be of allenic character. Additionally, all nitrile imines were reported to isomerize to the corresponding carbodiimides, both thermally and photochemically.

However, most studies directed to the use of tetrazoles as photoprecursors of reactive intermediates and unusual molecules are based on 2,5-disubstituted tetrazoles,[11,14−19] Even in 5-substituted tetrazoles, where the tetrazole ring bears a

Received: August 17, 2016
Published: November 3, 2016

DOI: 10.1021/acs.joc.6b02023
J. Org. Chem. 2016, 81, 11656−11663

labile hydrogen as substituent, it was observed that the 2*H*-tautomer was the predominant form isolated in the matrix,[14,17,19] in keeping with the behavior observed for the parent tetrazole.[20] Thus, the matrix photochemistry of 1,5-disubstituted tetrazoles remains mostly unexplored, apart from the work by Begué et al.[19] on the photolysis of 1-methyl-5-phenyltetrazole, where the formation of carbodiimide as the final photoproduct was demonstrated but no intermediates were detected. Although it could be expected that only the 2,5-disubstituted tetrazoles would give direct access to nitrile imines, we think that an investigation of the intermediates generated during photolysis of 1,5-disubstituted tetrazoles may add relevant information regarding the reactivity of the tetrazole chemotype and may also lead to new scaffolds.

Herein we report, for the first time, the intermediates generated from photolysis of a 1,5-disubstituted tetrazole in solid argon.

To better understand the effects of the ring substitution pattern on the photofragmentation pathways and species formed from disubstituted tetrazoles, the photolyses of the isomeric 1-methyl-5-aminotetrazole and 2-methyl-5-aminotetrazole were investigated, using similar experimental conditions.

Earlier photochemical studies of 2-methyl-5-aminotetrazole in solid argon[16,21] revealed the involvement of three different primary photochemical pathways: (1) tautomerization to mesoionic 3-methyl-1*H*-tetrazol-3-ium-5-aminide; (2) nitrogen elimination, with production of 3-amino-1-methylnitrilimine, which isomerize into 1-methyl-1*H*-diazirene-3-amine; (3) ring cleavage leading to methyl azide and cyanamide. Additionally, reactions of the primary photoproducts were observed, leading to methylenimine and hydrogen isocyanide.[16,21] Recent studies on the photochemistry of a small library of tetrazoles,[11,14−19] have demonstrated formation of nitrile imines and these intermediates were found to isomerize, forming carbodiimides as final products. However, in previous attempts to elucidate the photochemistry of 2-methyl-5-aminotetrazole, this isomerization was not observed. The coexistence of several possible routes, resulting in various photoproducts (some may result from more than one route), can easily lead to erroneous assignment of the IR absorptions.

We now discuss results of our investigation on the photochemistry of 1-methyl-5-aminotetrazole and 2-methyl-5-aminotetrazole using narrowband tunable UV-laser irradiation. This approach allows to induce the photoreactions of the isolated species selectively, providing data for further clarification of the photochemistry of these compounds. A comparison of the photochemistry of both isomers provides more information regarding the effects of the ring substitution pattern on the photofragmentation pathways of disubstituted tetrazoles. It is worth noting that 5-aminotetrazoles are important building blocks for the preparation of nitrogen-bridged saccharyl-tetrazole conjugates, a group of ligands that have demonstrated to act as selective copper chelators, affording copper complexes with cytotoxic properties.[22]

RESULTS AND DISCUSSION

Photochemistry of Matrix-Isolated 1-Methyl-5-aminotetrazole. As described in the Experimental Section, a sample of crystalline 1-methyl-5-aminotetrazole, **1a**, was sublimated under reduced pressure (at ≈60 °C), and the vapors of the compound were codeposited with argon (ca. 1:1000 molar ratio) onto a CsI substrate kept at 15 K. Figure 1a shows the infrared spectrum of **1a** isolated in solid argon in the 3600−2900 and 2500−800 cm^{-1} regions. The full mid-IR range spectrum of **1a** and the corresponding B3LYP/6-311++G(d,p) calculated spectrum are provided as Supporting Information, Figure S1.

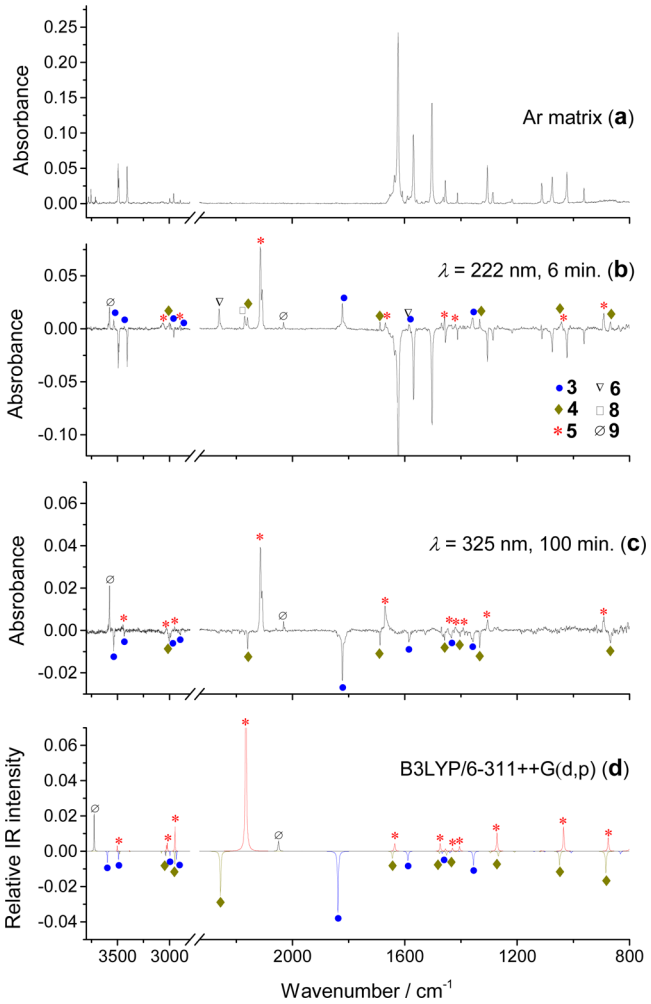

Figure 1. (a) Experimental IR spectrum of 1-methyl-5-aminotetrazole **1a** isolated in solid argon. (b and c) Difference IR spectra, showing spectral changes upon irradiation: (b) after 6 min of irradiation at λ = 222 nm (∼17 mW) of matrix **1a**; (c) after 100 min of irradiation at λ = 325 nm (∼22 mW), subsequent to the irradiation at λ = 222 nm for 6 min. In (c), the negative bands, blue circles and green rhombi correspond to the consumed diazirine **3** and cyanamide **4**, respectively. The bands with red stars correspond to carbodiimide **5**. (d) Theoretically calculated IR spectra of diazirine **3**, cyanamide **4**, carbodiimide **5**, and CNH **9**.

In order to investigate the photochemistry of **1a**, the deposited matrix was irradiated with UV light, as described in Experimental Section. The sample was monitored after each irradiation by recording its infrared spectrum.

Compound **1a** was irradiated with monochromatic UV-light at λ = 222 nm. Figure 1b shows the matrix spectrum of **1a** after irradiation for a total of 6 min, when around 60% of **1a** was consumed and photoproducts **3**−**9** were produced (see also Scheme 1). Photoproducts **3** (1822 cm^{-1}) and **4** (2159 cm^{-1}) appeared immediately after the first seconds of irradiation, followed by the increase of bands due to photoproduct **5** (2113/2107 cm^{-1}). Kinetic studies for the photolysis of **1a** (see Figure 2) indicated that the maximum amount of species **3** and

DOI: 10.1021/acs.joc.6b02023
J. Org. Chem. 2016, 81, 11656−11663

Scheme 1. Photochemistry of Matrix-Isolated 1a and 1b Was Induced by Using Monochromatic UV Light[a]

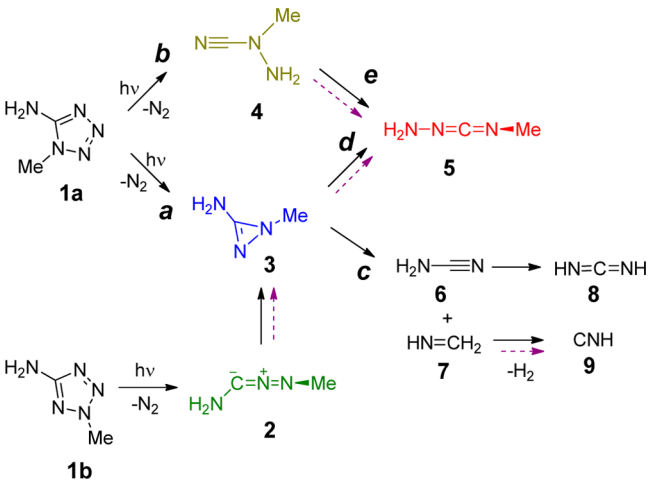

[a](a) Black plain arrows indicate the proposed pathways for the photolysis of tetrazoles **1a** and **1b**, at λ = 222 nm and λ = 250 nm, respectively, (b) violet dashed arrows indicate the proposed pathways when the matrix was irradiated at λ = 325 nm. Continuous irradiation of **1a** at λ = 222 nm activates two primary photochemical pathways, **a** and **b**, then three different secondary pathways **c**, **d**, and **e**. However, upon subsequent irradiation of the same matrix at λ = 325 nm, only pathways **e** and **d**, were observed. Continuous irradiation of **1b** at λ = 250 nm generates photoproduct **2**, which isomerizes into **3**, then decomposes through two different photochemical pathways, **c** and **d**. However, upon subsequent irradiation of the same matrix at λ = 325 nm, only isomerization of **2** into **3**, and pathway **d** were observed.

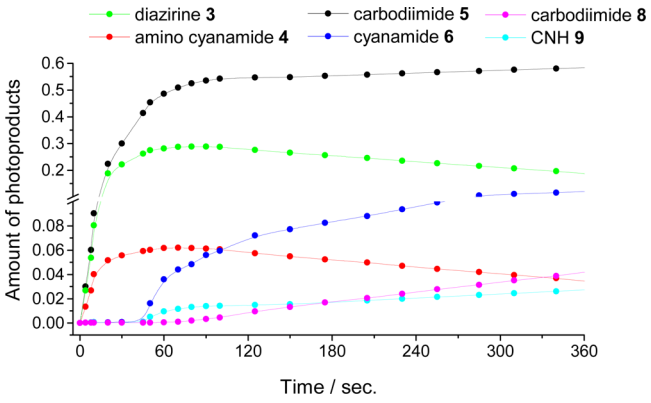

Figure 2. Kinetic profiles showing changes of populations of the photoproducts **3** (1822 cm^{-1}), **4** (2159 cm^{-1}), **5** (2113/2107 cm^{-1}), **6** (2261 cm^{-1}), **8** (2169 cm^{-1}), and **9** (2031 cm^{-1}) upon irradiation at λ = 222 nm of **1a**. In these profiles, the "amount of photoproducts" corresponds to the experimental integrated band intensities, with maxima at indicated frequencies. See the Experimental Section for details.

4 was reached after 60 s of irradiation at λ = 222 nm, and then started decreasing gradually, while bands due to photoproduct **5** kept increasing and those due two new photoproducts appeared. These new compounds were easily identified as cyanamide **6** (2261 cm^{-1}) and hydrogen isocyanide **9** (2031 cm^{-1}), based on previously reported IR spectra of these species in argon matrix.[14,23−26] Upon extended photolysis, new characteristic bands evolved, due to the isomerization of cyanamide **6** into carbodiimide **8** (2169 cm^{-1}), as previously reported.[23]

Proposed assignments for the infrared absorptions of **1a** and **1b**, and observed photoproducts **2**−**9**, are included as Supporting Information, Tables S1−S10.

The photoproducts **3** and **5** were readily identified as diazirine **3** and carbodiimide **5**. As will be disclosed in the next section, the same bands were observed from photolysis of isomer **1b** in solid argon. The identification of products **3** and **5** was supported by theoretical calculations and by data from previous photochemical studies of matrix-isolated tetrazoles.[14,15,17] On the other hand, the immediate increase of distinctive absorption bands at 2159 and 1688 cm^{-1} indicated the formation of an unknown primary photoproduct, **4**, obtained concomitantly with diazirine **3**. These results suggest that the formation of photoproducts **3** and **4**, occurring in the first stage of irradiation, involves two different pathways (**a** and **b**, respectively), both resulting from photocleavage of the tetrazole **1a**. Then, as secondary processes, three different pathways are observed: pathways **d** and **e** correspond, respectively, to the rearrangement of primary photoproducts **3** and **4** to carbodiimide **5**; pathway **c** involves the decomposition of diazirine **3** into cyanamide **6** (that undergoes subsequent isomerization into carbodiimide **8**, at λ = 222 nm) and hydrogen isocyanide **9**.

It is noteworthy that the elusive diazirine **3** is one of the few observations of antiaromatic 1*H*-diazirines. The capture of such antiaromatic (i.e., 4π systems) structures can be quite challenging, and has only been observed in a few cases, either upon isolation in cryogenic matrices of noble gases,[14,15,17,21,27,28] or in NMR monitored studies, at −50 °C.[29]

To gather further evidence regarding the photocleavage pathways involved, a new experiment was designed: after irradiation of tetrazole **1a** (at λ = 222 nm, 60 s), and generation of both photoproducts **3** and **4** in a maximal amount, we irradiated the matrix at λ = 325 nm, where the tetrazole **1a** was observed to be photostable but its photoproducts could be transformed. These irradiation conditions resulted in photoreactions of the primary photoproducts **3** and **4**, leading to formation of carbodiimide **5** in large amount, as sole photoproduct (see Figure 3, for kinetic profile). After 100 min of irradiation at λ = 325 nm, when all **3** and **4** were consumed, the bands corresponding to carbodiimide **5** remained unaltered, even at extended irradiation times, indicating that this compound is photostable under the conditions used.

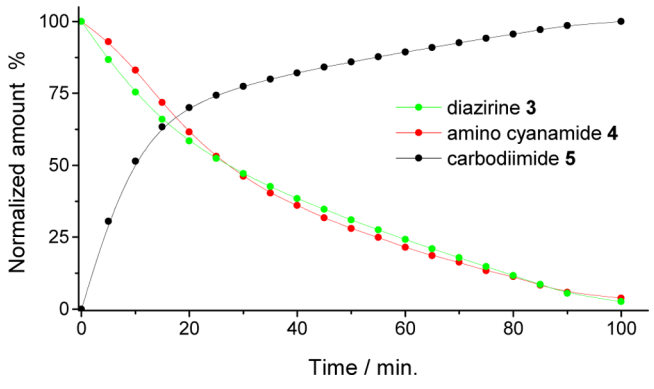

Figure 3. Kinetic profiles showing consumption of matrix-isolated diazirine **3** (1822 cm^{-1}) and amino cyanamide **4** (2159 cm^{-1}) and formation of carbodiimide **5** (2113/2107 cm^{-1}), upon irradiation at λ = 325 nm. See the Experimental Section for details.

DOI: 10.1021/acs.joc.6b02023
J. Org. Chem. 2016, 81, 11656−11663

Altogether, the experimental evidence shows that irradiation at λ = 222 nm activates three different secondary photochemical processes of decomposition of the primary photoproducts **3** and **4**: pathways **c**, **d**, and **e**. However, when a matrix containing the photoproducts **3** and **4** is irradiated at λ = 325 nm the photochemical pathway **c** is excluded, leading to a much cleaner spectrum (without the bands from photoproducts **6**–**9**). Figure 1c shows the different IR spectrum after irradiation at λ = 325 nm for 100 min, where we can observe the transformations of the primary photoproducts due to secondary photoreactions. The negative bands correspond to the consumed photoproducts **3** and **4** while the positive bands result from formation of photoproduct **5**. Thus, when irradiating at λ = 325 nm we can selectively activate pathways **d** and **e**, which involve photoisomerization of photoproducts **3** and **4** into carbodiimide **5**. The spectrum in Figure 1c also shows the formation of some CNH **9**, which will be explained below.

The unknown species **4** could be unambiguously identified as amino cyanamide from comparison between experimental and calculated IR spectra. The absorption bands expected for **4** above 800 cm^{-1} are clearly observed in Figure 1c (as green rhombi) and assigned in Table 1. The most characteristic band, at 2159 cm^{-1}, is assigned to the $\nu C{\equiv}N$ stretching mode, calculated at 2233 cm^{-1}. Also, a characteristic absorption at 1688 cm^{-1} fits the estimated vibration at 1627 cm^{-1}, which corresponds to the δNH_2 scissoring mode. The bands in the 1500–1400 cm^{-1} region correlate well with the calculated bands, and are assigned to the three δCH_3 bending modes. The band calculated at 1038 cm^{-1} could not be ascribed with certainty, though it seems to correspond mainly to one of the CH_3 rocking modes, appearing overlapped with the mixed $\nu NN/wNH_2$ vibration of carbodiimide **5**, observed in the experimental spectrum at 1042 cm^{-1}. As can be seen in Figure 1c, in the experimental difference IR spectrum resulting from the photochemistry of both **3** and **4** upon irradiation at λ = 325 nm, such superposition results in nearly cancelation of both bands (from the consumed reagent **4** and the formed product **5**). The experimental absorption bands above 2900 cm^{-1} were assigned to the antisymmetric νNH_2 (3431 cm^{-1}) and νCH_3 (3054, 3008, and 2918 cm^{-1}) stretching vibrations, although some of the assignments shall be considered as tentative. Indeed, the bands due to the CH_3 stretching modes appearing in this spectral range are expected to have very low intensity, and the overlap of absorptions from both photoproducts (**4** and **5**) is also expectable, since they have similar predicted νNH_2 and νCH_3 stretching frequencies (see Tables S5 and S6 in Supporting Information). All other bands of photoproduct **4**, observed at 1333 (νN_7C_6), 1185 (νN_7C_1; wNH_2), 1133 ($\gamma CH_3'$), and 868 (wNH_2) cm^{-1}, nicely fit with the calculated data (see Table 1).

Table 1. Proposed Band Assignments for the Observed IR Bands of Photoproduct Amino Cyanamide 4 (Argon Matrix; 15 K), and B3LYP/6-311++G(d,p) Calculated Vibrational Wavenumbers (ν,cm^{-1}) and IR Intensities (I, km mol^{-1}) for This Molecule[a,b]

	Ar matrix		calculated	
approximate description	ν	I[c]	ν	I
νNH_2 as	3431	11	3445	9.2
νNH_2 s			3346	1.9
νCH_3 as″	3054	22	3044	7.2
νCH_3 as′	3008	22	3004	16.3
νCH_3 s	2918	17	2919	48.2
$\nu C{\equiv}N$	2159	67	2233	161.6
δNH_2	1688	45	1627	25.6
δCH_3 as″	1463	39	1461	8.5
δCH_3 as′	1434	22	1437	14.5
δCH_3 s	1403	11	1404	2.5
γNH_2			1281	6.2
νN_7C_6	1333	50	1254	18.1
νN_7C_1; wNH_2	1185	17	1197	3.2
$\gamma CH_3'$	1133	17	1107	2.2
$\gamma CH_3''$	1042	45	1038	49.7
wNH_2	868	62	875	80.5

[a]Calculated wavenumbers were scaled by 0.968. [b]ν, stretching; δ, bending; γ, rocking; w, wagging; s, symmetric; as, antisymmetric. The primes in the approximate description of the methyl group vibrations refer to local symmetry of the mode, under assumption of methyl local C_s symmetry. [c]Experimental intensities, after 60 s of irradiation at λ = 222 nm, were obtained from the measured absorbances, by normalization to the total intensity of the observed counterparts.

Concerning pathway **c**, it should be noted that the formation of cyanamide **6** could in principle result from either the cleavage of the tetrazole **1a**, generating cyanamide and methyl azide, or from cleavage of the diazirine **3**, generating cyanamide **6** and methylenimine **7**. However, its formation via cleavage of the tetrazole **1a** can be ruled out, since no evidence of methyl azide in the photolyzed matrix could be found. According to the available spectroscopic data, the νNNN antisymmetric mode of methyl azide gives rise to an intense absorption band around 2100 cm^{-1}.[30] This expected intense band could not be observed, although we need to consider that it could be overlapped by the intense band due to carbodiimide **5**, at 2113/2107 cm^{-1}. Besides, several new bands could in principle also be assigned to the methyl azide. However, after irradiations at λ = 325 nm, where the **1a** does not react and no formation of methyl azide should be observed, these same bands kept increasing, providing clear indications that they belong to other photoproducts, and excluding the presence of methyl azide as putative photoproduct in the photolyzed matrix. This observation indicates that the formation of cyanamide **6** arises exclusively from photolysis of diazirine **3**, which can suffer a ring-opening photoreaction leading to cyanamide **6** and methylenimine **7**. It is well-known that the photodecomposition of matrix isolated methylenimine **7** gives rise to hydrogen isocyanide **9** by 1,1-H_2 elimination.[25,26] Also, evidence for the presence of these species (cyanamide **6**, methylenimine **7**, and hydrogen isocyanide **9**) was observed only after formation of diazirine **3**. We could assign some of the observed bands to methylenimine **7**, although the assignment of bands due to this compound is tentative due to the low intrinsic intensities of the bands of this species (see Table S8). However, formation of the photoproduct **9** was observed beyond doubt and, according to the available knowledge regarding the photochemistry of **7**, one can then expect that the formation of **9** should result essentially from the presence of methylenimine **7** in the matrix.

As previously explained, formation of cyanamide **6** was not observed upon irradiation at λ = 325 nm, suggesting that, at this wavelength, pathway **c** can be ruled out. However, as can be observed in Figure 1c, irradiation at λ = 325 nm led to formation of a small amount of hydrogen isocyanide **9**. We propose that this compound results from photodecomposition

DOI: 10.1021/acs.joc.6b02023
J. Org. Chem. 2016, 81, 11656–11663

of the remaining methylenimine **7**, obtained in the first stage of irradiation, at λ = 222 nm.

The identification of the photoproducts was supported by results of earlier investigations regarding the photochemistry of the parent 5-amino tetrazole[14] and of 2-methyl-5-amino-tetrazole **1b**,[16,21] under low-temperature matrix-isolation conditions. In fact, a comparison between the observed bands in the photolysis of tetrazole **1a** and the ones reported from earlier studies for the photolysis of the isomer **1b**, reveals excellent correlation among several absorption bands, a clear evidence that the same photoproducts, **3** and **6**–**9**, were obtained in both cases. However, the previous studies on 2,5-substituted tetrazole **1b** failed in the correlation of one expected species, the carbodiimide **5**. In the previous investigations on the photolysis of **1b**, several absorption bands were assigned to a methyl azide (including the distinguishable bands at 2113/2017 cm^{-1}) and different photodegradation pathways were proposed, but the carbodiimide **5** was excluded as final photoproduct.

In view of these inconsistencies, we decided to reinvestigate the photolysis of **1b** using narrow band UV irradiation, which, as demonstrated above for **1a**, can be expected also in this case to allow inducing selective photoconversion of the initially formed photoproducts of **1b** without consuming this latter species. This procedure can help clarify the details of the photochemistry of the compound.

Photochemistry of Matrix-Isolated 2-Methyl-5-amino-tetrazole. Figure 4b shows the IR spectra of the matrix-isolated **1b** after irradiation at λ = 250 nm (~40 mW) for total of 4 s, when around 50% of **1b** was consumed, and bands corresponding to six different species were detected: photo-products **2**, **3**, **5**–**7**, and **9**. These photoproducts were readily identified as nitrile imine **2**, diazirine **3**, carbodiimide **5**, cyanamide **6**, methylenimine **7**, and hydrogen isocyanide **9** based on the previously described results for the photolysis of **1a** and on data reported from earlier studies on the photolysis of **1b**.[16,21] Indeed, in view of the generation of diazirine **3** as intermediate from the photolysis of both isomers **1a** and **1b**, it is reasonable to expect the same channels of photo-fragmentation of diazirine **3**, with formation of photoproducts **5**–**9** (pathways **c** and **d**) upon photolysis of both isomers. There is, however, one relevant difference: in the case of isomer **1b**, the diazirine **3** results from photoisomerization of nitrile imine **2**, detected during our experiments. The formation of cyanamide **6** and methylenimine **7** could result from either the photofragmentation of diazirine **3**, as previously described for the photolysis of **1a**, or directly form nitrile imine **2**, as was observed for the parent unsubstituted 5-aminotetrazole.[14] However, during photolysis of **1b** the bands due to cyanamide **6** were only observed after formation of diazirine **3**, and kept increasing even after total consumption of nitrile imine **2** (see the kinetic profiles in Figure 5), in keeping with the results obtained from the photolysis of **1a**, where we never observed any evidence of formation of nitrile imine species. It should also be noted that the formation of carbodiimide **8** was only observed in a separate experiment, when a matrix containing the photoproduct cyanamide **6** was irradiated at λ < 230 nm.

In summary the nitrile imine **2** (1963/1937 cm^{-1}) is the main species generated in the first second of irradiation, starting to be consumed after two seconds of irradiation with concomitant increase of diazirine **3** (1822 cm^{-1}), followed by photoproducts: cyanamide **6** (2261 cm^{-1}), hydrogen isocyanide **9** (2031 cm^{-1}), and carbodiimide **5** (2113/2107 cm^{-1}).

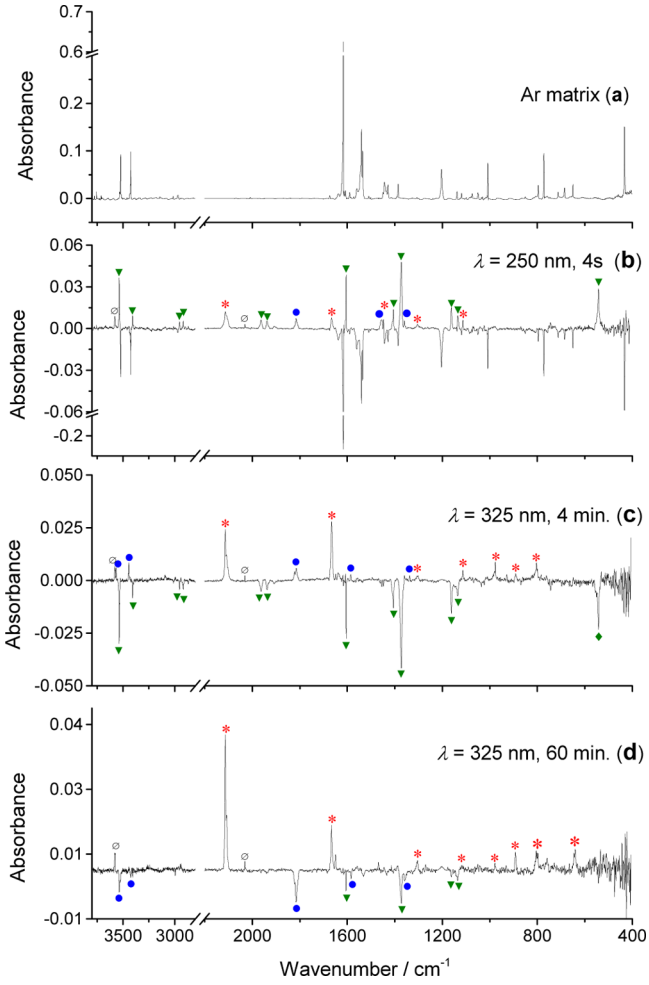

Figure 4. (a) Experimental IR spectrum of 2-methyl-5-aminotetrazole **1b**, in solid argon at 15 K. (b, c, and d) Difference IR spectra in solid argon showing spectral changes: (b) after 4 s of UV irradiation at λ = 250 nm (~40 mW) of matrix isolated **1b**; (c) after 4 min of irradiation at λ = 325 nm (~22 mW) subsequently to the irradiation of 4 s at λ = 250 nm. In (c) the negative bands with olive triangles correspond to the consumed nitrile imine **2**. The blue circles and red stars are assigned to diazirine **3** and carbodiimide **5**, respectively; (d) after +60 min of irradiation at λ = 325 nm, subsequently to the 4 min of irradiation under the same conditions.

Irradiations of this same solid matrix at λ = 325 nm, where **1b** remains photostable, resulted in two different observations (see the experimental IR in Figure 4 and the kinetic profiles in Figure 6): (i) during the first 4 min of irradiation all the nitrile imine **2** is consumed, with concomitant increase of diazirine **3** and carbodiimide **5**; (ii) after the first 4 min of irradiation, the bands due to diazirine **3** start to decrease, with concomitant growth of those due to carbodiimide **5**, as sole photoproduct, until all the diazirine **3** is consumed. As observed during photolysis of the isomer **1a**, when the matrix containing the photoproduct **3** (from isomer **1b**) was irradiated at λ = 325 nm the photochemical pathway **c** was excluded.

These results unequivocally demonstrate that the 5-amino tetrazole **1b** follows the photofragmentation patterns observed for other 2*H*-tetrazoles, with generation of nitrile imine **2** by extrusion of N_2, followed by its photoisomerization into diazirine **3** that also photoisomerizes to carbodiimide **5** as final photoproduct.[11,14−19] As previously reported, the experimental IR bands at 1963 and 1937 cm^{-1} due to the

DOI: 10.1021/acs.joc.6b02023
J. Org. Chem. 2016, 81, 11656−11663

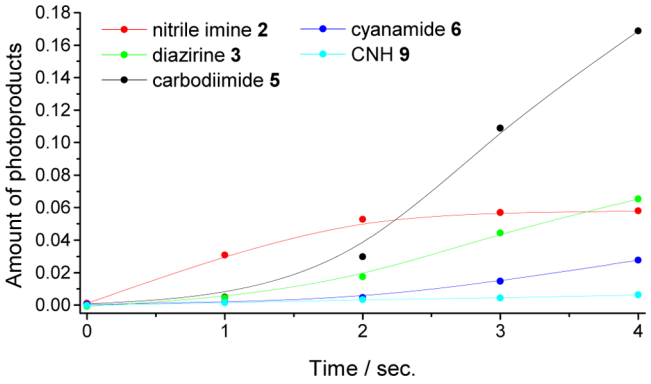

Figure 5. Kinetic profiles showing changes of populations of the photoproducts **2** (1963 cm^{-1}) **3** (1822 cm^{-1}), **5** (2113/2107 cm^{-1}), **6** (2261 cm^{-1}), and **9** (2031 cm^{-1}), upon irradiation at λ = 250 nm of matrix-isolated **1b**. In these profiles, the "amount of photoproducts" corresponds to the experimental integrated band intensities, with maxima at indicated frequencies. See the Experimental Section for details.

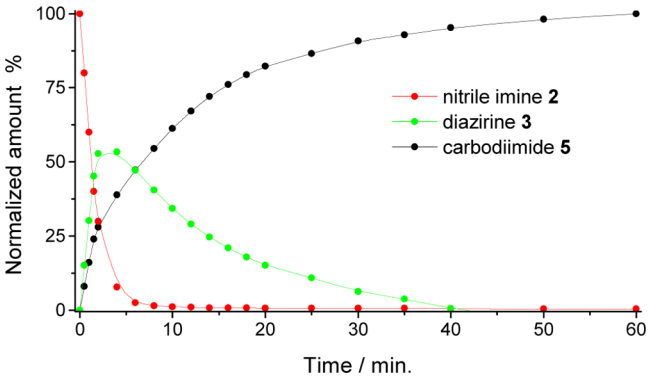

Figure 6. Kinetic profiles showing changes of matrix-isolated nitrile imine **2** (1963 cm^{-1}) to carbodiimide **5** (2113/2107 cm^{-1}) via diazirine **3** (1822 cm^{-1}) upon irradiation at λ = 325 nm. See the Experimental Section for details.

νCNN antisymmetric stretching, suggests a significant carbenic character of the amino nitrile imine **2**.[16] These results are in agreement with the ones obtained for the parent C-amino nitrile imine (which was ascribed to bear a contribution of around 20% of the carbenic resonance hybrid).[14]

In contrast, during the photolysis of **1a** we never observed any evidence of formation of a nitrile imine species, even after carefully searching for evidence during the first few seconds of irradiation (when usually the nitrile imine are known to be observed). This result may mean that only 2*H*-tetrazoles could provide direct access to nitrile imines. The formation of amino cyanamide **4** from UV-irradiation of isomer **1a**, observed for the first time from photolysis of tetrazoles under low temperature matrices, is also a relevant result of the present investigation.

CONCLUSIONS

We isolated compounds **1a** and **1b** in solid argon and studied their matrix photochemistry.

Photolysis of matrix-isolated **1a** at λ = 222 nm results in species **3**–**9**, obtained in two stages. The photoproducts diazirine **3** and amino cyanamide **4** are obtained in a first stage of irradiation (primary photoproducts), through two different pathways, both resulting from the photocleavage of tetrazole **1a**. In a second stage two different pathways are observed, involving isomerization of both diazirine **3** and amino cyanamide **4** into carbodiimide **5**. Also a third pathway is observed, involving decomposition of diazirine **3** into photoproducts **6**–**9**. However, with subsequent irradiations of the matrix containing compounds **3** and **4** at λ = 325 nm, we could prevent decomposition of diazirine **3** and exclude this last photochemical pathway, simplifying the interpretation of the experimental spectra and rendering the interpretation of the photochemical pathways easier.

Photolysis of matrix-isolated **1b** at λ = 250 nm results in products, **2**, **3**, **5**–**7**, and **9**, which were obtained in two stages. The nitrile imine **2** is the main species generated in the first second of irradiation, isomerizing readily into diazirine **3** (also obtained from photolysis of the matrix-isolated isomer **1a**). These results unequivocally demonstrate that the amino tetrazole **1b** follows the same photofragmentation patterns observed for other 2*H*-tetrazoles, with generation of nitrile imine, by extrusion of N_2, its photoisomerization into diazirine that subsequently photoisomerizes to give carbodiimide as final product.

Interestingly, we found that the photochemistry of the two isomers, **1a** and **1b**, although resulting in the same intermediate diazirine **3**, which undergo subsequent photoconversion into carbodiimide **5**, seems to follow different pathways. In fact, the amino cyanamide **4** was exclusively obtained from photocleavage of the isomer **1a**, whereas the nitrile imine **3** was exclusively obtained during the photolysis of **1b**. This exclusive formation of nitrile imine from the isomer **1b** could mean that only the 2*H*-tetrazoles forms can give a direct access to nitrile imines.

We could assign the vibrational absorptions of the various photoproducts and propose the different photochemical pathways. However, the mechanistic pathway for formation of the species **4** upon irradiation of isomer **1a** is not clear. We postulate the formation of nitrene species, which could have different structures, with only the one resulting from **1a** enabling formation of aminocyanamide **4**. This could explain the different photochemical pathways observed for isomers **1a** and **1b**. Further research is needed to clarify this last point.

EXPERIMENTAL SECTION

General Information. The chemicals used were of analytical grade and were used without further purification. When required, solvents were freshly distilled from appropriate drying agents before use. The solvents for extraction were of technical grade. Melting points recorded are uncorrected. Mass spectra were obtained by electron ionization (EI) at 70 eV. NMR (400 MHz) spectra were measured using TMS as the internal reference (δ = 0.0 ppm).

Preparation of Compounds. Methyltetrazole-5-amines (**1a**, **1b**) were prepared through methylation of commercially available 5-aminotetrazole monohydrate, as previously described.[31]

1-Methyl-(1*H*)-tetrazole-5-amine (1a). Colorless needles (6.1 g; 51% yield), mp 220–221 °C (lit, 220 °C[31]); ^{1}H NMR (400 MHz, $CDCl_3$): δ 4.15 (3H, s); MS (EI): *m*/*z* 99 $[M]^+$.

2-Methyl-(2*H*)-tetrazole-5-amine (1b). Colorless needles (3.0 g, 25% yield), mp 104–105 °C (lit, 104 °C[31]); ^{1}H NMR (400 MHz, $CDCl_3$): δ 3.32 (3H, s); MS (EI): *m*/*z* 99 $[M]^+$.

Matrix Preparation, Infrared Spectroscopy. The matrix was prepared by codeposition of the matrix gas (argon, 99.9998%, obtained from Air Liquid) and vapors of the tetrazole under analysis (**1a** or **1b**) produced by sublimation onto the cooled CsI substrate of the cryostat in a specially designed variable-temperature mini-oven assembled inside the cryostat. The cryogenic system was based on a closed-cycle helium refrigeration system with a DE-202A expander. The temperature of the CsI substrate during deposition was 15 K. The infrared

DOI: 10.1021/acs.joc.6b02023
J. Org. Chem. 2016, 81, 11656–11663

spectra of matrix-isolated compounds were obtained using a Fourier transform infrared spectrometer equipped with a deuterated triglycinesulfate (DTGS) detector and a Ge/KBr beam splitter with 0.5 cm^{-1} spectral resolution.

UV-Laser Irradiation Experiments. The matrix was irradiated through the outer quartz window of the cryostat using a narrow band (fwhm ~0.2 cm^{-1}) with the frequency-doubled signal beam of a Quanta-Ray MOPO-SL optical parametric oscillator, pumped with a pulsed Nd:YAG laser (repetition rate = 10 Hz, pulse energy ≈1−5 mJ, duration = 10 ns). The UV light used to induce the initial photochemistry of **1a** and **1b** was selected according to the UV−vis spectra obtained in ethanol at room temperature, which show an absorption maximum at ~222 nm and ~248 nm, respectively. (See Figure S2 in Supporting Information)

Theoretical Calculations. Quantum-chemical calculations were performed with density functional theory using the valence triple-ζ polarized 6-311++G(d,p) basis set[32,33] and the B3LYP functional.[34,35] The optimization of geometries was followed by harmonic vibrational calculations undertaken at the same level of theory. The calculated harmonic vibrational frequencies were scaled by a factor of 0.968 obtained by least-squares linear fit of the experimental versus calculated frequencies of **4** (Figure S3, Supporting Information). The calculated frequencies were then used, to simulate the spectra using Lorentzian functions with fwhm equal to 4 cm^{-1} and to assist the analysis of the experimental spectra. All of the calculations were performed with the Gaussian 09 suite of programs.[36]

Kinetic Measurements. Figure 2 shows one experiment where the species isolated in the matrix were irradiated for a total amount of 6 min, at λ = 222, when around 60% of **1a** was consumed and several different photoproducts (**3**−**9**) were formed. Figure 3 shows a different experiment where the first irradiation was performed at λ = 222 nm, to generate the maximum amount of diazirine **3** and amino cyanamide **4**. During this experiment, generation of **5** and **6** was also observed. The outset of the kinetics in Figure 3 corresponds to the end (60 s) of the previous irradiation (λ = 222 nm). For the second part of the experiments, with irradiation at λ = 325 nm, the relative amounts of **3**, **4**, and **5** were assumed as 100, 100, and 0%, respectively. After 100 min, **3** and **5** were completely consumed, and the produced amount of **5** was set to 100%. Figure 5 shows one experiment where the species isolated in the matrix were irradiated for a total amount of 4 s at λ = 250, when around 50% of **1b** was consumed and several different photoproducts (**2**, **3**, **5**, **6**, and **9**) were formed. The aim of the experiment performed with irradiation at λ = 250 nm was to produce the maximum amount of nitrile imine **2**. Generation of species **3**, **5**, and **6** was also observed. The outset of the kinetics in Figure 6 corresponds to the end of the previous irradiation (λ = 250 nm). For the experiments carried out with irradiation at λ = 325 nm, the relative amounts of **2**, **3**, and **5** were assumed as 100, 0, and 0%, respectively. After 60 min of this irradiation, **2** and **3** were completely consumed, and the generated amount of **5** was set to 100%. At 4 min, the total amount of **2** and **5** was ~46.7% and achieved the bottom. The residual was parametrized to 53% as the maximal amount of **3** generated. All the amounts of species shown in Figures 2, 3, 5, and 6 correspond to the experimental integrated band intensities, with maxima at indicated frequencies.

■ ASSOCIATED CONTENT

Supporting Information

The Supporting Information is available free of charge on the ACS Publications website at DOI: 10.1021/acs.joc.6b02023.

Least-squares linear fit of the experimental versus calculated frequencies of **4**; figures showing UV−vis and experimental and calculated IR spectra of 1-methyl-5-aminotetrazole **1a** and 2-methyl-5-aminotetrazole **1b**; proposed band assignments for the infrared spectrum of **1a**, **1b**, and relevant photoproducts **2**−**9**; Cartesian coordinates and electronic energies for all optimized structures at the B3LYP/6-311++G(d,p) level (PDF)

■ AUTHOR INFORMATION

Corresponding Authors

*E-mail: rfausto@ci.uc.pt

*E-mail: mcristi@ualg.pt

Notes

The authors declare no competing financial interest.

■ ACKNOWLEDGMENTS

The authors gratefully acknowledge Fundação para a Ciência e a Tecnologia (FCT), and FEDER/COMPETE 2020-UE, through projects UID/Multi/04326/2013 (Centre of Marine Sciences - CCMAR), UI0313/QUI/2013 (Coimbra Chemistry Centre - CQC), PTDC/MAR-BIO/4132/2014, and PTDC/QEQ-QFI/3284/2014 − POCI-01-0145-FEDER-016617. A.I. thanks FCT for financial support through grant SFRH/BD/90435/2012.

■ REFERENCES

(1) Yu, Z.; Ohulchanskyy, T. Y.; An, P.; Prasad, P. N.; Lin, Q. *J. Am. Chem. Soc.* **2013**, *135* (45), 16766−16769.

(2) Shi, H.; Zhang, C. J.; Chen, G. Y. J.; Yao, S. Q. *J. Am. Chem. Soc.* **2012**, *134* (6), 3001−3014.

(3) Lim, R. K. V; Lin, Q. *Acc. Chem. Res.* **2011**, *44* (9), 828−830.

(4) Li, Z.; Qian, L.; Li, L.; Bernhammer, J. C.; Huynh, H. V.; Lee, J. S.; Yao, S. Q. *Angew. Chem., Int. Ed.* **2016**, *55* (6), 2002−2006.

(5) Zhao, S.; Dai, J.; Hu, M.; Liu, C.; Meng, R.; Liu, X.; Wang, C.; Luo, T. *Chem. Commun.* **2016**, *52* (25), 4702−4705.

(6) Zhu, B.; Ge, J.; Yao, S. Q. *Bioorg. Med. Chem.* **2015**, *23* (12), 2917−2927.

(7) Tasdelen, M. A.; Yagci, Y. *Angew. Chem., Int. Ed.* **2013**, *52* (23), 5930−5938.

(8) Wang, Y.; Song, W.; Hu, W. J.; Lin, Q. *Angew. Chem., Int. Ed.* **2009**, *48* (29), 5330−5333.

(9) Song, W.; Wang, Y.; Qu, J.; Madden, M. M.; Lin, Q. *Angew. Chem., Int. Ed.* **2008**, *47* (15), 2832−2835.

(10) Song, W.; Wang, Y.; Qu, J.; Lin, Q. *J. Am. Chem. Soc.* **2008**, *130* (30), 9654−9655.

(11) Maier, G. G.; Eckwert, J. J.; Bothur, A.; Reisenauer, H. P.; Schmidt, C. *Liebigs Ann.* **1996**, *1996* (7), 1041−1053.

(12) Frija, L. M. T.; Cristiano, M. L. S.; Gómez-Zavaglia, A.; Reva, I.; Fausto, R. *J. Photochem. Photobiol., C* **2014**, *18*, 71−90.

(13) Frija, L. M. T.; Ismael, A.; Cristiano, M. L. S. *Molecules* **2010**, *15* (5), 3757−3774.

(14) Nunes, C. M.; Reva, I.; Rosado, M. T. S.; Fausto, R. *Eur. J. Org. Chem.* **2015**, *2015* (34), 7484−7493.

(15) Nunes, C. M.; Reva, I.; Fausto, R.; Bégué, D.; Wentrup, C. *Chem. Commun.* **2015**, *51*, 14712−14715.

(16) Baskir, E. G.; Platonov, D. N.; Tomilov, Y. V.; Nefedov, O. M. *Mendeleev Commun.* **2014**, *24* (4), 197−200.

(17) Nunes, C. M.; Araujo-Andrade, C.; Fausto, R.; Reva, I. *J. Org. Chem.* **2014**, *79* (8), 3641−3646.

(18) Pagacz-Kostrzewa, M.; Mucha, M.; Weselski, M.; Wierzejewska, M. *J. Photochem. Photobiol., A* **2013**, *251*, 118−127.

(19) Bégué, D.; Qiao, G. G.; Wentrup, C. *J. Am. Chem. Soc.* **2012**, *134* (11), 5339−5350.

(20) Bugalho, S. C. S.; Maçôas, E. M. S.; Cristiano, M. L. S.; Fausto, R. *Phys. Chem. Chem. Phys.* **2001**, *3* (17), 3541−3547.

(21) Gómez-Zavaglia, A.; Reva, I. D.; Frija, L.; Cristiano, M. L.; Fausto, R. *J. Phys. Chem. A* **2005**, *109* (35), 7967−7976.

(22) Ismael, A. L.; Henriques, M. S. C.; Marques, C.; Rodrigues, M.; Barreira, L.; Paixão, J. A.; Fausto, R.; Cristiano, M. L. S. *RSC Adv.* **2016**, *6* (75), 71628−71637.

(23) Duvernay, F.; Chiavassa, T.; Borget, F.; Aycard, J.-P. *J. Phys. Chem. A* **2005**, *109* (4), 603−608.

(24) King, S. T. *J. Chem. Phys.* **1971**, *54* (3), 1289.

(25) Milligan, D. E.; Jacox, M. E. *J. Chem. Phys.* **1963**, *39* (3), 712.

DOI: 10.1021/acs.joc.6b02023
J. Org. Chem. 2016, 81, 11656−11663

(26) Jacox, M. E.; Milligan, D. E. *J. Mol. Spectrosc.* **1975**, *56* (3), 333−356.
(27) Ismael, A.; Borba, A.; Henriques, M. S. C.; Paixão, J. A.; Fausto, R.; Cristiano, M. L. S. *J. Org. Chem.* **2015**, *80* (1), 392−400.
(28) Gómez-Zavaglia, A.; Reva, I.; Frija, L.; Cristiano, M.; Fausto, R. *J. Mol. Struct.* **2006**, *786* (2−3), 182−192.
(29) Dubau-Assibat, N.; Baceiredo, A.; Bertrand, G. *J. Am. Chem. Soc.* **1996**, *118* (22), 5216−5220.
(30) Milligan, D. E. *J. Chem. Phys.* **1961**, *35* (4), 1491.
(31) Ismael, A.; Paixão, J. A.; Fausto, R.; Cristiano, M. L. S. *J. Mol. Struct.* **2012**, *1023* (null), 128−142.
(32) Frisch, M. J.; Pople, J. A.; Binkley, J. S. *J. Chem. Phys.* **1984**, *80* (7), 3265.
(33) Krishnan, R.; Binkley, J. S.; Seeger, R.; Pople, J. A. *J. Chem. Phys.* **1980**, *72* (1), 650.
(34) Gill, P. M. W.; Johnson, B. G.; Pople, J. A.; Frisch, M. J. *Chem. Phys. Lett.* **1992**, *197* (4−5), 499−505.
(35) Becke, A. D. *Phys. Rev. A: At., Mol., Opt. Phys.* **1988**, *38* (6), 3098−3100.
(36) Frisch, M. J.; Trucks, G. W.; Schlegel, H. B.; Scuseria, G. E.; Robb, M. A.; Cheeseman, J. R.; Scalmani, G.; Barone, V.; Mennucci, B.; Petersson, G. A.; Nakatsuji, H.; Caricato, M.; Li, X.; Hratchian, H. P.; Izmaylov, A. F.; Bloino, J.; Zheng, G.; Sonnenberg, J. L.; Hada, M.; Ehara, M.; Toyota, K.; Fukuda, R.; Hasegawa, J.; Ishida, M.; Nakajima, T.; Honda, Y.; Kitao, O.; Nakai, H.; Vreven, T.; Montgomery, J. A., Jr.; Peralta, J. E.; Ogliaro, F.; Bearpark, M.; Heyd, J. J.; Brothers, E.; Kudin, K. N.; Staroverov, V. N.; Kobayashi, R.; Normand, J.; Raghavachari, K.; Rendell, A.; Burant, J. C.; Iyengar, S. S.; Tomasi, J.; Cossi, M.; Rega, N.; Millam, J. M.; Klene, M.; Knox, J. E.; Cross, J. B.; Bakken, V.; Adamo, C.; Jaramillo, J.; Gomperts, R.; Stratmann, R. E.; Yazyev, O.; Austin, A. J.; Cammi, R.; Pomelli, C.; Ochterski, J. W.; Martin, R. L.; Morokuma, K.; Zakrzewski, V. G.; Voth, G. A.; Salvador, P.; Dannenberg, J. J.; Dapprich, S.; Daniels, A. D.; Farkas, O.; Foresman, J. B.; Ortiz, J. V.; Cioslowski, J.; Fox, D. J. *Gaussian 09*, Revision A.02; Gaussian, Inc.: Wallingford, CT, 2009.

DOI: 10.1021/acs.joc.6b02023
J. Org. Chem. 2016, 81, 11656−11663